Pozuelo, J., Fernández-Carretero, F. J., Riande, E., Saiz, E. & Compañ, V. (2008): Comparison Between the Conductivities of Protons Measured Experimentally with the Obtained by Molecular Dynamics Simulations in Sulfonated Polyphenyl Sulfones Membranes. *Journal of New Materials for Electrochemical Systems*, 11 (2), pp.: 87-94.

Comparison Between the Conductivities of Protons Measured Experimentally with the Obtained by Molecular Dynamics Simulations in Sulfonated Polyphenyl Sulfones Membranes

Javier Pozuelo[1], F. J. Fernández-Carretero[2], Evaristo Riande[3], Enrique Saiz[4] and *Vicente Compañ[2]

[1]Departamento de Materiales, ETSII, Universidad Carlos III, Madrid, Spain
[2]Departamento de Termodinámica Aplicada, ETSII, Universidad Politécnica de Valencia, 46022-Valencia, Spain [3]Instituto de Ciencia y Tecnología de Polímeros (CSIC), 28006 Madrid, Spain
[4]Departamento de Química Física, Facultad de Ciencias, Universidad de Alcalá, Alcalá de Henares, Madrid, Spain

Full Molecular Dynamics was used to simulate separately the diffusion of naked protons and H_3O^+ hydrated protons across sulfonated polyphenyl sulfones, (sPS). The diffusion coefficient of naked protons is nearly one order of magnitude higher than that of the hydrated protons for the membranes with the lower water uptake (10%). The conductivities simulated at 300 K for the hydrated proton across membranes with water uptake 18% and 30 % are roughly similar to those both experimentally measured for the sPS4 membrane with ion exchange capacity = 1.8 eq/Kg in dry conditions and with water uptake = 24.3 %. The comparison between four sPS membranes shwon the strong dependence of conductivity with the water content into the membranes. In our study, the conductivity of sPS1 with a 3.1% water content decrease two order of magnitude respect the sPS4 with 24.3 of water content. Simulated conductivities of both naked protons and hydrated protons follow Arrhenius behavior.

Keywords: Proton conductivity, Molecular simulation, Polysulfone, Diffusion coefficient

1. INTRODUCTION

Polymers or ionomers with ionic groups attached in their structure are indispensable electrolyte materials for a great number of electrochemical applications such as, ionic exchange membranes for electrodyalisis, fuel cells of kind PEMFC and DMFC, batteries, sensors, that are already outlined as a future alternative energy source [1-3].

The first synthetic ion-exchange membranes were reported in the 1950s [4, 5]. Since then, a great variety of ion-exchange membranes have been prepared as a result of the ever-increasing use of these materials in separation processes, synthesis of high purity substances, batteries, fuel cells, etc. Good performance ion-exchange membranes for a variety of applications should exhibit high ionic permselectivity, high ionic conductance, low permeability to free diffusion of electrolytes and low electroosmosis, as well as chemical stability, mechanical resistance, flexibility and good dimensional stability in working conditions [6-8]. Nevertheless, some of these properties are incompatible. For example, high mechanical resistance requires thick membranes, which is incompatible with high conductance. High ion exchange capacity increases permselectivity and conductance, but it may be a negative factor for both dimensional stability and mechanical resistance. From a practical point of view, good performance membranes must exhibit a suitable balance of incompatible properties.

The synthesis of cation-exchange membranes that combine low protonic resistance and good mechanical properties in adverse operating conditions is nowadays a flourishing field of research [9]. Although perfluorocarbon polymers conveniently sulfonated are the best materials that meet these requirements, their still high cost and negative environmental effects make necessary to look for alternative materials. In principle, polymers with high chemical stability and good mechanical properties, such as polysulfones, polyimides, polyether ketones, etc., are suitable materials to prepare acidic membranes [9].

The main problem of the proton exchange membrane for use in

*To whom correspondence should be addressed: Email: vicommo@ter upv es
Tel : +34963879328, Fax: +34963877329

fuel cell (PEMFC) is the control of the water balance within the cell. Besides, it is well known that the properties and water content of the membrane play important roles in the processes dominating the cell performance. In this sense, it is known that the conductivity of the membranes decreases about three o more orders of magnitude when the water content into the polyelectrolyte is less than 30% [10,11]. Therefore, it is important to understand the transport phenomena of water in the membrane and its influences. Many theoretical studies have been developed to describe the water transport in this kind of membranes to apply on cell performance [12-16]. Their results illustrate the importance of water transport but the majority of the models concentrate on the analysis under steady-state conditions. However, the transient transport behaviors in a polyelectrolite are still for solving basically in mobile systems. Recently F. Chen et al. [17] have developed a one-dimensional mathematical model to describe the water transport in a PEMFC where both steady state and transient cell operation conditions are investigated with the consideration for the swelling effect of the membrane caused by the membrane hydratation. Their results provide more physical insights on water transport behaviors of a PEMFC and benefit the practical application and design work as well, but never is indicated who is the mechanism of water transport in the MEA and how is the proton diffusion in cation-exchange membranes, because it is not a well understood phenomenon. This process presumably involves dissociation of the proton from the acidic site, subsequent transfer of the proton to the aqueous medium, screening by water of the hydrated proton from the conjugated base or fixed anion, and finally diffusion of the proton in the confined water within the polymer matrix [18]. Therefore, the dependence of proton mobility on water content is quite critical, and demands effective cell and stack design to maintain a high level of water through the thickness of the membrane for the complete range of dynamic operation. It is worth noting that both evaporation and electro-osmotic drag processes severely diminish membranes humidification at typical working temperatures of fuel cells causing a significant increase of the protonic resistance.

Theoretical studies of polymer electrolytes through molecular dynamics are important for the design of good performance conducting membranes. Realistic models of ionic salts for polyethylene oxide-inorganic salt (for example NaI) suggest that the ions in the conductive process slide along a polymer chain by breaking bonds between ions and polymer segments and renewing these bonds with other segments of the same or another polymer [19-21]. Accordingly there is a strong coupling between ion motion and segmental relaxation in such a way that an understanding of ionic conduction in polyelectrolytes requires a detailed knowledge of segmental relaxations in these systems. Models have been reported that depict particle motion as hopping between neighboring sites or ion coordinating sites on a two-dimensional lattice. Chain motions are simulated by periodically redistributing or "repercolating" the hopping paths at relaxation times t_r in such a way that the model relates the dependence of ion transport on polymer motion [22].

In this work, the trajectories of naked protons and hydrated protons (H_3O^+) in sulfonated polyphenyl sulfone membranes are simulated using full dynamics techniques at different temperatures lying in the range 300 – 360K. Once the trajectories reach Einstein behavior, the diffusion coefficients of the protons are determined from which the conductivities are obtained. The simulations were carried out for polysulfone cation exchange membranes with different water content, keeping the ion exchange capacity constant, and the results for the conductivity obtained were further compared with experimental results.

2. EXPERIMENTAL PART

2.1. Sulfonation of polysulfones

Polyphenylsulfone Radel R-5000 was sulfonated with trimethylsilylchlorosulfonic acid using a procedure reported elsewhere [23-25]. The membranes were prepared by casting of the functionalized polyphenylsulfones in -methyl pyrrolidone solutions.

Schemes of the repeating units of the functionalized polysulfone chains are shown in Figure 1. The degree of sulfonation was determined by elemental analysis and titration with a 0.01M hydroxide sodium solution. Small differences between the two methods were found (less than 2%). The mean values of these results were 12, 45, 67 and 86 for sPS1, sPS2, sPS3 and sPS4, respectively.

2.2. Water uptake and proton exchange capacity

Dried membranes in the acidic form were weighed and further immersed in distilled water overnight. Then the membranes were gently pressed between filter paper and weighed again. The number of molecules of water per ion-exchange site is given in table 1.

Cation exchange membranes were obtained by casting from sulfonated polyphenyl sulfone solutions. The ion-exchange capacity of the membranes (IEC) was obtained by both titration and elemental

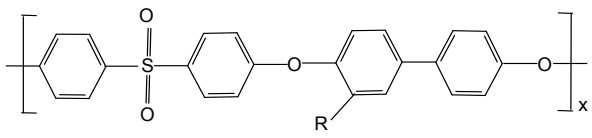

Figure 1. Repeating unit of the polyphenylsulfone Radel®. R = SO_3H for membranes in the acidic form with sulfonic fixed groups.

Table 1. Water uptake and ion-exchange capacity of the polyphenyl sulfone membranes containing sulfonic groups in their structure. Characteristics of the membranes involving geometric dimensions used in conductivity measurements. Resistance, electrical conductivity and

Membrane	Surface (cm^2)	Thickness (cm)	Wt (%)	Degree of sulfonation	IEC[a] (eq/g)	IEC[b] (eq/g)	R_0 (W)	$s\times10^{+5}$ S/cm	n1	n2
sPS1	0.7854	0.0045	3.1	12	0.28	0 30	625	0.23	0.77	-
sPS2	0.7854	0.0067	6.7	45	0.77	0.81	498	1.35	0.75	0.71
sPS3	0.7854	0.0079	8.8	67	1.31	1 25	550	1.69	0.78	0.64
sPS4	0.7854	0.0112	24.3	86	2.06	1.99	90	35.6	0.80	-

analysis (EA). The membranes were soaked in acidic form with 1 M sodium chloride solution for one week to convert the membrane from the H^+ form to Na^+ form. The protons released in the ion-exchange reaction $R\text{-}SO_3H + Na^+ \rightarrow R\text{-}SO_3Na + H^+$ were titrated with a sodium hydroxide solution in order to obtain the ion exchange capacity whose values are given in table 1. Elemental analysis was conducted in a LECO CHNS-932, values obtained are given in the same table 1.

3. PROTONIC RESISTANCE

Complex impedance measurements were performed in the frequency range $10^{-2} < f < 10^7$ Hz with 0.1V amplitude. The membranes previously equilibrated with water were placed between two gold electrodes coupled to a Novocontrol Broadband Dielectric Spectrometer (Hundsangen, Germany) integrated by a SR 830 lock-in amplifier with an Alpha dielectric interface. The temperature was controlled by nitrogen jet (QUATRO from Novocontrol) with a temperature error of ≈ 0.1 K during every single sweep in frequency. Membranes were sandwiched between the electrodes in a BDS 1308 liquid sample cell filled with distilled water to simulate a 100% RH atmosphere.

The conductivity of the membranes was obtained from impedance measurements using the equivalent circuit of figure 2a and 2b, respectively, depending on the experimental results. In the equivalent circuit we have the protonic resistance R_0 of the membrane in series with a circuit made up of an element R_1 that represents the charge transfer resistance at the membrane/electrode interface in parallel with a constant phase element representing the membrane/electrode double layers connected in series. When the result gave two arcs the conductivity was analized following the circuit of figure 2b, where other resistence, R_2, in parallel with other constant phase element representing the interfaces boundary layers is introduced. By assuming that the phase element admittance is $Y^*=Y_0(j\omega\tau)^n, 0 < n \leq 1$, the complex impedance of the circuit 2b is given by

$$Z = R_0 + \frac{R_1}{1 + R_1 (j\omega\tau_1)^{n_1}} + \frac{R_2}{1 + R_2 (j\omega\tau_2)^{n_2}} \tag{1}$$

where τ_l (i=1,2) is the relaxation times associated with the two process which taken place into the system membrane-solution and boundary layers and w the frequency. When only an arc is obtained the real and imaginary part of the impedance are given by

$$Z' = R_0 + \frac{R_1\left[1 + Y_0(\omega\tau_0)^n \cos\frac{n\pi}{2}\right]}{1 + Y_0^2(\omega\tau_0)^{2n} + 2Y_0(\omega\tau_0)^n \cos\frac{n\pi}{2}} \tag{2}$$

and

$$Z'' = j\omega L - \frac{R_1 Y_0 (\omega\tau_0)^n \sin\frac{n\pi}{2}}{1 + Y_0^2 (\omega\tau_0)^{2n} + 2Y_0 (\omega\tau_0)^n \cos\frac{n\pi}{2}} \tag{3}$$

where ω is the frequency and τ_0 is a characteristic relaxation time. Notice that in the limits $\omega \rightarrow \infty$ and $\omega \rightarrow 0$, $Z' \rightarrow R_0$ and $Z' \rightarrow R_0 + R_1$, respectively. In the limit $\omega \rightarrow 0$, $Z'' \rightarrow 0$, but the only way that $Z'' \rightarrow 0$ at $\omega \rightarrow \infty$ is that $L = 0$. If inductive effects

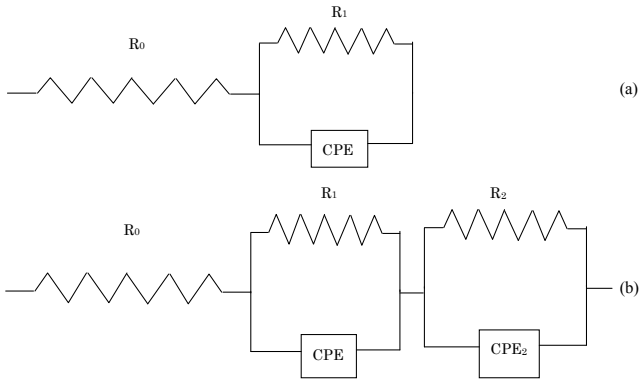

Figure 2. Equivalent circuit showing the protonic resistance of a membrane in series with a parallel RC circuit containing a constant phase element that accounts for the departure of the relaxation behavior of the membrane from Debye behaviour.

are absent, the Z'' *vs* Z' plot (Nysquit diagram) [26], gives a curve that intersects the abscissa axis at $Z' = R_0$, at high frequencies. Also, since lim $|Z^*| \rightarrow R_0$ and $\tan^{-1}(Z''/Z') \rightarrow 0$ in the limit $\omega \rightarrow \infty$, where $|Z^*|$ is the modulus of the complex impedance, from the plots of both $|Z^*|$ and $\tan^{-1}(Z''/Z')$ *vs* ω the protonic resistance is obtained [27].

The value of R_0 leads to the protonic conductivity s using the following expression

$$\sigma = \frac{l}{R_0 A} \tag{4}$$

were A and *l* are, respectively, the area and thickness of the membranes.

4. MEAN SQUARE DISPLACEMENTS AND PROTONIC DIFFUSION

The relationship between conductivity and ionic diffusion in cation-exchange membranes can be obtained using Nernst Planck ionic transport formalism. In a cation-exchange membrane partially or totally equilibrated with water, electric current under a unidirectional electric force field, dψ/dx, is transported by counterions, the diffusion coefficient, D_+, is related with the conductivity by mean of the expression

$$\sigma = -\frac{j}{d\psi / dx} = F z_+ c_+ \overline{u}_+ = \frac{F^2 z_+^2 c_+ D_+}{RT} \tag{5}$$

where *F* is Faraday's constant, c_+ and z_+ are, respectively, the concentration of the counterion and its valence and RT has the usual meaning.

Eq.(5) can be expressed in a more conventional way for simulation calculations by

$$\sigma = \frac{N_+ z_+^2 e^2 D_+}{VkT} \tag{6}$$

Where N_+ is the number counterions in the simulation box of volume V, *k* is the Boltzmann constant and *T* is the absolute tem-

perature. The conductance is often written as

$$\sigma = \frac{N_+ z_+^2 e^2 D_+}{VkTH_R} \tag{7}$$

where $H_R = D_+/D_{s+}$ is Haven ratio, a factor that compensates for ion correlations, and D_{s+} is the actual diffusive conductivity. In the simulations H_R was set to 1 [28].

In molecular terms, the diffusion coefficient can be obtained from either the velocity or displacement of each diffusing particle along the trajectories and further averaging over all time origin and over all particles, thus, the diffusion coefficient can be computed from the velocity autocorrelation function or kubo formalism.

Other method is the so-called Einstein relation in which the diffusion coefficient D_+ of counterions in a cation-exchange membrane can be calculated by the mean-square displacement

$$D_+ = \frac{1}{6N_+}\lim_{t\to\infty}\frac{d}{dt}\sum_{i=1}^{N}\left\langle\left[\mathbf{R}_+(t)-\mathbf{R}_+(0)\right]^2\right\rangle \tag{8}$$

The sum term on the right hand side of eq(8) over N_+ is called the mean square displacement (MSD). N_+ is the number of diffusing counterions, t is time and $\mathbf{R}_+(t)$ is the position vector of a counterion at time event *t*. Average MSD-curves as a function of time for each diffuser type are calculated. It is essential to notice that Eq. (8) is only valid when the Einstein diffusion is reached. This means that the motion of the diffusing particle follows a random walk, in other words, its motion is not correlated with its motion at any previous time. To test the region in which the Eq. (8) is valid, log(MSD) against log(t) was plotted in each case. The slope of the curve is 1±0.03 [29], when the Einstein diffusion is reached:

$$\frac{\Delta\log(MSD)}{\Delta\log(t)} = 1 \tag{9}$$

The primary simulation involves the generation of starting structures of the polymer in a box which properly represent the entirety of the polymer sample. For that purpose MD methods have been used and are well described in the literature [30-32].

The advance of each particle inside the cell arises from the force field of the polymeric systems which in its simplest form can be written as a sum of terms, each one of them representing a different kind of interaction:

$$E_{pot} = E_{bon} + E_{ang} + E_{rot} + E_{vdW} + E_{cha} + E_{oop} + ... \tag{10}$$

where the terms in the sum represent, respectively, energies due to bond stretching, angle bending, intrinsic rotational barriers, van der Waals interactions, Coulombic interactions, out of plane bending, and any other kind of interaction that may take place within the studied sample. In the simplest case the force field of the can be written as

$$E_{pot} = \sum_{bonds}\frac{k_{ij}}{2}(b_{ij}-b_{ij}^0)^2 + \sum_{angles}\frac{k_{ijk}}{2}(\theta_{ijk}-\theta_{ijk}^0)^2 + \sum_{rotations}\frac{k_\phi}{2}\left[1+\frac{|s|}{s}\cos(|s|\phi)\right] + \sum_{i,j}\frac{A_{ij}}{r_{ij}^{12}} - \frac{B_{ij}}{r_{ij}^6} + \sum_{i,j}\frac{q_i q_j}{\varepsilon r_{ij}} \tag{11}$$

where k_{ij} and b_{ij}^0 represent the force constant and the unstressed length that are characteristic for the kind of bond joining those two atoms. In a similar way, k_{ijk} and θ_{ijk}^0 represent the force constant for angles deformation and the angle unstressed, respectively. The third sum gives the intrinsic torsional potential energy functions, and finally the two last terms corresponds to the van der Waals and Coulombic interactions. Here qi represent the partial atomic charges and ε is the dielectric constant of the medium. For a system of N atoms in the Cartesian coordinates r_i(i=1,2,…,N) with potential energy $E_p = E_p(r_i)$ the evolution of the system along a path of constant energy can be obtained by solving Newton's equation of motion.

$$\frac{d^2 r_i}{dt^2} = -\frac{1}{m_i}\frac{\partial E_p}{\partial r_i} = \frac{F_i}{m_i} \tag{12}$$

The eq.(12) is solved numerically by using discretization for the second order differential operator on the left hand side. The most frequently used procedure for MD calculations consists in employing the same approach used for the numerical integration of any general function f(x), namely to replace the actual function by a stair function. The algorithm used by us in this work for the integration of the equation of motion has been the leap frog algorithm [33,34].

4.1. Computational details

Bulk structures of poly(ether sulfone) with sulfonic acid anions and water absorbed were generated and simulated by using the Accelrys commercial software (Materials Studio 3.2) [35] using the PCFF91 force field [36].

Membranes were built by constructing 3D amorphous cells containing different amounts of polymer, water and diffusion particles, using the Amorphous_cell module made by Accelrys Inc with five chains of ten units of poly(ether sulfone) (PES10) (Figure 1) and different amounts of H+, H_3O+ and H_2O. The cells called cellA, cellB and cellC of Table 2 contain naked protons whereas cellD cellE and cellF contain hydrated protons (H_3O^+). The amount of water was 10 wt% in cellA and cellD; 18wt% in cellB and cellE; and 30wt% in cellC and cellF.

The PCFF force field [37-41] was developed to model polymers, but it has been found also suitable for modeling PES with sulfonic acids [42]. Charges were calculated by QEq_charged 1.1 available in Materials Studio software. The six structures were first minimized by Conjugate Gradient method for 5,000 steps until the maximum derivative was less than 0.1 Kcal/(Å mol). A 200 ps long MD run using NVT ensemble was performed with a time step of 1

Table 2. Description of the different simulated cells. Each cell have five chains of ten units of poly(ether sulfone) (PES10) and different amounts of H^+, H_3O^+ and H_2O described in table.

Cell	Number of				Wt% of water	Density (g/cm^3)
	PES10	H_2O	H^+	H_3O^+		
A	5	135	50	0	10	1.32
B	5	240	50	0	18	1.29
C	5	400	50	0	30	1.26
D	5	85	0	50	10	1.32
E	5	190	0	50	18	1.29
F	5	350	0	50	30	1.26

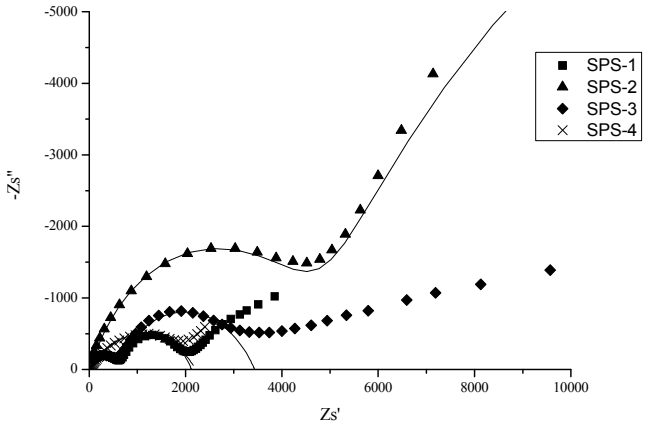

Figure 3. Nyquist diagram for sPS1, sPS2, sPS3 and sPS4 membranes equilibrated with water at 300K. The continuous line indicate the ajust of experimental values following the circuit shown in figure 2.

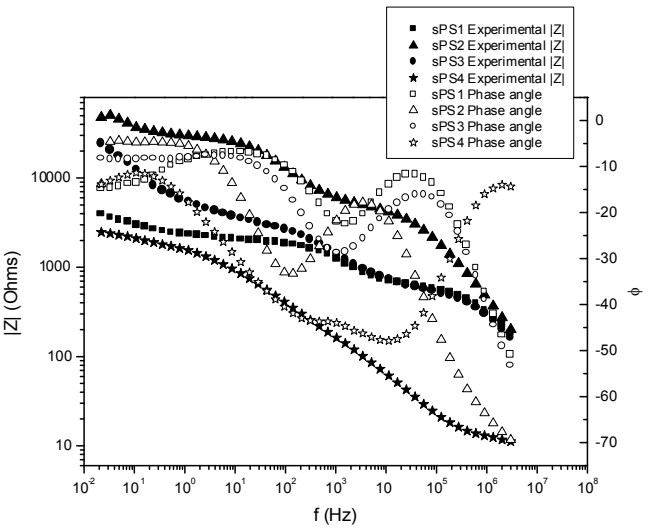

Figure 4. Impedance module in Ohms and phase angle versus frequency,(Bode diagram), for the same membranes ploted in figure 3, equilibrated with distilled water.

fs. For properly calculations, a MD run of 2 ns was performed using the constant-NVT ensemble with a time step of 1 fs. Trajectories were saved each 500 fs for subsequent analysis. Periodic boundary conditions were used in all calculations. The Van der Waals and coulombic non-bonding interactions were calculated by the cell multipole method (CMM) [43-45]; the value of the update width parameter was 1.0 Å and the accuracy parameter was set to Medium to use 3rd order in the Taylor series expansion and explicit interactions form more neighboring cells. The structural results obtained by using the fast CMM methods for the cells agree with the results obtained with the slow Ewald summation method [46]. In all systems, the temperature was 300, 320, 340 and 360 K and was controlled by the Andersen thermostat method with a collision ratio of 1.0. In this work we assumed a constant density in the range of 300 to 360 K.

5. RESULTS AND DISCUSSION

Complex plots of the components of the complex impedance obtained for the sPS membranes equilibrated with water are shown in figure 3. The Nyquist diagrams are arcs in the high region frequency intersecting with the abscissa axis at $Z'=R_0$. Departure of semicircles is observed at lower frequencies as a result of polarization processes and other phenomena taking place in the membrane electrode interface. Alternative Bode diagrams are shown in figure 4 for all membranes experimentally studied. The plots show a plateau at high frequencies coexisting with the peak of the out of phase angle *f* where its value is close to 0, of the complex impedance. The modulus of the impedance at the peak maximum was taken as the protonic resistance R_0 of the membranes. Table 1 shows the values of the protonic resistances that we used to calculate the conductivity by mean of eq.(4). These values of the conductivity of the membranes at 300 K are also given in the last column of table 1.

The interpretation of the experimental results in terms of the equivalent circuit containing a constant phase element, figure 2-a, shows that eq.(2) and (3) fit the complex plots by assuming that n=0.7-0.8 for the membranes sPS1 and sPS4. In case of sPS2 and sPS3 membranes we used the equivalent circuit showed in figure 2-b. The exponent of the phase element in the circuits accounts for the complexity of the polarization processes in such way that the higher the complexity, the lower the n. The values of n and the conductivity for the sPS membranes at 300K, at 100% of humidity, are shown in table 1. In general, the values of the proton conductivity follow the same trends as the ion-exchange capacity, in the sense that the membrane with higher value of this latter quantity (sPS4) exhibits the highest conductivity. The correlation is not so good with the ion capacity per g of water uptake. Thus the values of $[H^+]/cm^3$ H_2O in the membrane phase for sPS4 and sPS1 membranes are, respectively, 6.55×10^{-3} and 6.15×10^{-3}, whereas the conductivities at 300 K are 3.56×10^{-4} S/m and 0.23×10^{-5} S/m, respectively. These results suggest that membranes with high water uptake facilitate chains mobility that in turn makes easier carriers jumping between fixed membrane anions thus decreasing ohmic resistance.

There is a vivid debate concerning both the nature of the water in wet ion-exchange membranes and the proton transport mechanism. Studies carried out by Paddison et al. [47-50] on the dielectric spectrum of Nafion and PEEK in the microwave region showed a strong dependence between proton conductivity and water content. This dependence is weaker for PEEK membranes owing to the stronger confinement of water in the narrow channels of these membranes. The confinement of the water in nanodimensional domains under a strong electrostatic field arising from the dissociated fixed ionic groups seems to keep the water molecules more tightly bound to each other and to the anionic fixed groups, thus inhibiting the structural diffusion of the protons. Moreover, they point out that hydrogen bonding between the sulfonic acid groups is favored, and it is likely that a minimal amount of water in the membrane forms a continuous path through which protons can diffuse.

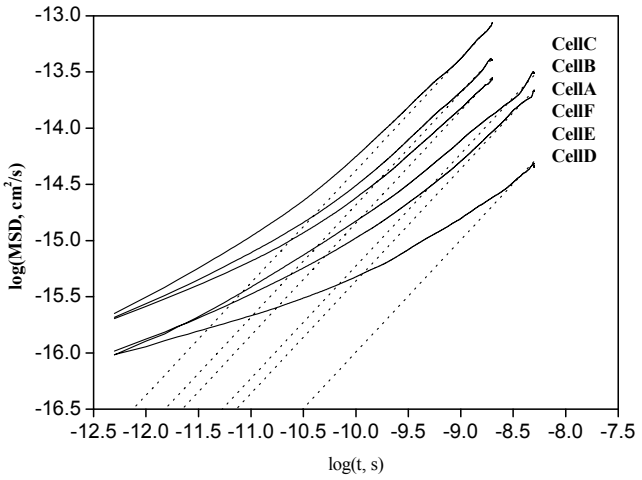

Figure 5. Mean Square Displacement of H^+ (cells A, B and C) and H_3O^+ (D, E and F) as a function of time, at 300 K.

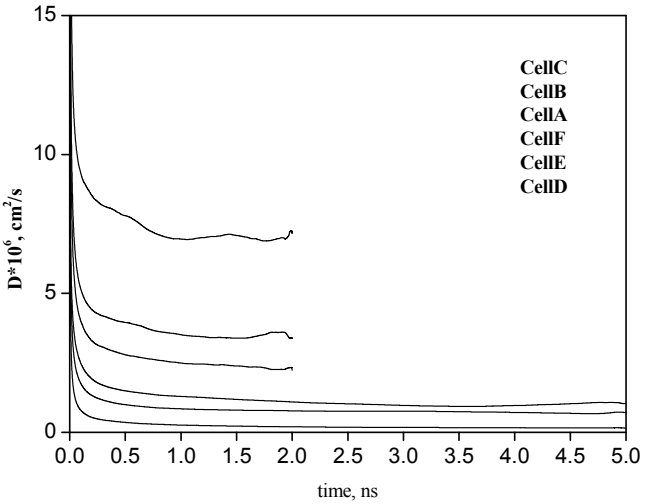

Figure 6. Evolution of the diffusion coefficient, in cm^2/s, with time in ns for H^+ (cells A, B and C) and H_3O^+(cells D, E and F).

Theoretical models have been developed focused in the elucidation of ion transport in ion-exchange membranes. In these models, certain amount of coarse-graining in the form of phenomenological parameters has been introduced. For example, Eikerling et al [24] developed a phenomenological model where the mobility of the protons is assumed to proceed via structure diffusion along the array of the anions of fixed groups over the interface, and a bulk mechanism where the protons are transported by the Grottus mechanism.

We have addressed proton transport in cation-exchange membranes using full dynamics considering the diffusion of naked protons and the hydrated H_3O^+ particle. Possible formation of hydrophilic and hydrophobic domains is implicit in the conformational space landscape. Simulated protonic MSD values for cells A, B and C, at four temperatures, are shown as a function of time in Figure 5. As expected, the values of MSD increase with time and temperature, the plots being straight lines of slopes close to unit in the whole time range. When the time is large enough, the diffusive regime is reached and $<[\mathbf{R}_+(t) - \mathbf{R}_+(0)]^2>$ varies linearly with time, i.e. the slope of the $\log<[\mathbf{R}_+(t) - \mathbf{R}_+(0)]^2>$ vs. log(t) plot reaches unity and the diffusion coefficient may be obtained from eq (9). Values of the diffusion coefficient of single protons are plotted as a function of time in Figure 6. All the curves show a sharp decrease of the diffusion coefficient with increasing time in the low times region and the value of this quantity remains nearly constant at both moderate and long times. The values simulated for D_+ at different temperatures for three cells with different water content are collected in the second, fourth, sixth and eighth columns of Table 3. It can be seen that the diffusion coefficient of protons inside the membranes increases with both temperature and water content of the cells. Values of the conductivity calculated using the results simulated for D_+ by eq(7) are given in the third, fifth, seventh and ninth columns of Table 3. The simulated conductivity is nearly one order of magnitude larger than the experimental result. The conductivity roughly follows Arrhenius behavior as the plots of Figure 7 show. In this figure we plot the simulated D, E, and F cells and experimental values for the sPS4 membranes for comparison. The activation energies was about of 2 or 2.5 Kcal/mol for the cells simulated and around 3 Kcal/mol for the sPS4 membranes, whose characteristics were similar to the simulated cells. A common characteristic of the results of Table 3 is that the protonic transport is associated with a low activation energy which in the most unfavorable cases is lower than three kcal mol^{-1}. The energy is higher

Table 3. Simulated values of the diffusion coefficient, D_+, in cm^2/s, at different temperatures for the six cells simulated and described in table II. The electrical conductivity, σ, in S/cm, is obtained following the eq.(6).

Cell	Temperature, K							
	300		320		340		360	
	$10^6 \times D$	$10^3 \times \sigma$	$10^6 \times D$	$10^3 \times \sigma$	$10^6 \times D$	$10^3 \times \sigma$	$10^6 \times D$	$10^3 \times \sigma$
A	2.32	21.4	3.05	26.4	4.79	39.1	4.92	37.9
B	3.49	29.4	6.50	52.0	8.13	60.4	8.73	61.3
C	6.99	52.5	9.90	69.7	14.19	94.0	16.83	104.4
D	0.167	1.54	0.310	2.69	0.346	2.83	0.349	2.70
E	0.720	6.08	1.01	7.98	1.160	8.65	1.45	10.2
F	0.987	7.57	1.22	8.74	2.18	14.7	2.25	14.4

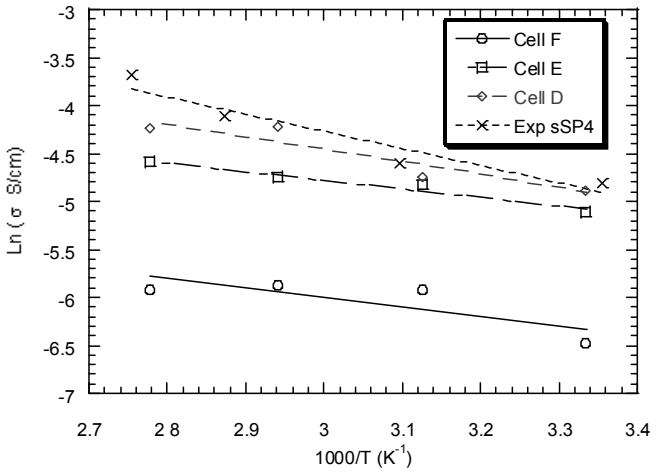

Figure 7. Arrhenius plots for the conductivity, in S/cm, of H_3O^+ (cells D, E and F) and sPS4 membrane.

than that predicted by Synder et al based on the dynamic of bond percolation [22], but lower than the experimental values reported for proton conduction in polylelectrolytes.

Let us consider now the full molecular dynamics for the diffusion of hydrated protons H_3O^+ across membranes using the data of the cell D, E and F of Table 2. The trajectories for hydrated protons in Figure 5 are similar to those found for naked protons. Semi logarithmic plots of the RMS of H_3O^+ shown as a function of time at different temperatures, exhibit the same behavior as the naked protons in the sense that present a transitory process followed by steady state conditions. The diffusion coefficient experiences a sharp drop with increasing time at short times, this coefficient remaining constant at moderate and long times such as it can be shown in figure 6. As expected, the association of a proton with a molecule of water slows down the diffusion process of the hydrated particle and the conductivity simulated for membranes with water uptake 18% and 30% is roughly similar to that experimentally found for membrane sPS4. Finally, the temperature dependence of the conductivity depicted in Figure 7 show that this parameter for H_3O^+ also follows Arrhenius behavior with low activation energy similar in all cases and roughly similar to found for sPS4 membranes with similar water content and ionic exchange capacity.

6. CONCLUSIONS

The diffusion of naked protons in sulfonated phenyl polysulfones is nearly one order of magnitude larger than hat of the hydrated protons. The value of the conductivity simulated for H_3O^+ is roughly similar to that experimentally found. Simulated conductivities of hydrated protons follow Arrhenius behaviour, but the activation energy is lower than that experimentally found for cation-exchange membranes. Although the rather good agreement between simulated and experimental conductivities for similar water content of the sPS membranes is stimulating, more work must be carried out in polyelectrolytes with different chemical structures to asses the reliability of full molecular dynamics to predict proton conductivities of cation-exchange membranes as a function of the chemical structure. The comparison between the sPS membranes showed the strong dependence of conductivity with the water content into the membranes, for example in our study the conductivity of sPS1 with a 3.1% water content decrease two order of magnitude respect the sPS4 with 24.3 of water content.

7. ACKNOWLEDGEMENTS

This work was supported by the Dirección General de Investigación Científica y Técnica (DGICYT), Grant MAT-2005-05648-C02-02, and from IMPIVA of Generalitat Valenciana through project IMCITA/2006/030 is gratefully acknowledged. The authors are also grateful to the Instituto de Tecnología Eléctrica (ITE) de la Universidad Politécnica de Valencia for the financial support.

REFERENCES

[1] N. Miyake, J.S. Wainright, R.F. Savinell, J. Electrochem. Soc., 148, A898 (2001).

[2] G.Alberti, M.Casciola, Annu. Rev. Mater. Res., 33, 129 (2003).

[3] M. Ulbricht, Polymer, 47, 2217 (2006).

[4] Wyllie J. R., Patnode H. W., J. Phys. Chem., 54, 204 (1950).

[5] Juda W., McRae W.A., J. Am. Chem. Soc., 72, 1044 (1950).

[6] N Demineralization by Electrodyalisis, J. Wilson, ed., Butterworths, London, 1960.

[7] Lakshminarayanaiah, N. Transport Phenomena in Membranes, Academic Press, London, 1967.

[8] Riande E. in Physics of Electrolytes, Vol 1, Academic Press, 1972; Chapter 11.

[9] Hickner M. A., Ghassemi H., Kim Y. S., Einsla B.R., McGrath J. E., Chem., 104, 4587 (2004).

[10]M. A. Hickner, H. Ghassemi, Yu Seung Kim, B. R. Einsla, J. E. McGrath, Chem., 104, 4587 (2004).

[11]Carla Heitner-Wirguin, J. Membr. Sci., 120, 1 (1996).

[12]G. J. Elfring, H. Struchtrup, J. Membr. Sci., 297, 190 (2007).

[13]Trung V. Nguyen, R. E. White., J. Electrochem. Soc., 140, 2178 (1993).

[14]V. Mishra, F. Yang, R. Pitchumani, J. Power Sources, 141, 47 (2005).

[15]Jung S. Yi, Trung V. Nguyen, J. Electrochem. Soc., 145, 1149 (1998).

[16]T. Okada, G. Xie, Y. Tanabe, J. Electroanal. Chem., 413, 49 (1996).

[17]Falin Chen, Min-Hsing Chang, Chi-Fu Fang, J. Power Sources, 164, 649 (2007).

[18]Paddison S. J., Ann. Mat. Res., 33, 289 (2003).

[19]Neyertz S., Brown D. J., Chem. Phys., 104, 3797 (1996).

[20]Müller-Plathe F., van Gunsteren W. F., J. Chem. Phys., 103, 4745 (1995).

[21]Leeuw, S.W., van Zon A., Bel G., J. Electrochim. Acta, 46, 1419 (2001).

[22]J. F. Synder, M. A. Ratner, D. F. Shriver, Solid State Ionics, 147, 249 (2002).

[23]Parcero E., Herrea R., Nunes S., J. Memb. Sci., 285, 206 (2006).

[24]Dyck A., Fritsch D., Nunes S. P., J. Appl. Polym. Sci., 86, 2820 (2002).

[25]Jakoby K., Nunes S.P., Peinemann, (GKSS) Patent application, DE 101 48 131.4 (09/28/2001).

[26]H. Nyquist, Phys., 32, 110 (1928).

[27]W. W. Bode, Network Analysis and Feedback Amplifier Design, Van Nostrand, Princenton, N.J. 1956.

[28]M. C. Lonergan, Ion Transport in Polymer Electrolytes, PhD Thesis, Northwestern University, Evanston, IL, 319 (1994).

[29]Müller-Plathé F., Acta. Polym., 45, 259 (1994).

[30]D. V. Heermann, Computer Simulation Methods in Theoretical Physics, 2nd ed. Springer-VerlayBerlin Heildelberg, 1990.

[31]M. P. Allen and D. J. Tildesley, Computer Simulation of Liquids., Clarendeon Press, Oxford, 1987.

[32]R. J. Roe, Computer Simulation of Polymers, Printice Hall, Englewood Cliffs, N.J. 1991.

[33]E. Riande and E. Saiz, Molecular dynamics: a powerful tool for the evaluation of conformational dielectric properties of polymer chains. Current Trends in Polymer W science., Vol 2, 1997.

[34]J. Pozuelo, E. Riande, E. Saiz, and V. Compañ, Macromolecules, 39, 8862 (2006).

[35]Accelrys Inc, San Diego, CA USA (Materials Studio 3.2, VISUALIZER, AMORPHOUS CELL and DISCOVER modules).

[36]Sun H, Mumby S. J., Maple J. R., Hagler A. T., J. Am. Chem. Soc., 116, 2978 (1994).

[37]Sun H., J. Comput. Chem., 15, 752 (1994).

[38]Sun H., Macromolecules, 28, 701 (1995).

[39]Hill J-R, Sauer J., J. Phys. Chem., 98, 1238 (1994).

[40]Maple J.A., Hwang M.J., Stockfisch T.P., Dinur U, Waldman M., Ewig C.S., Hagler A.T., J. Comput. Chem., 15, 162 (1994).

[41]Sun H, Mumby S.J., Maple J.R., Hagler A.T.. J. Am. Chem. Soc., 116, 2978 (1994).

[42]Ennari J., Hamara J., Sundholm F., Polymer, 38, 3733 (1997).

[43]Greengard L., Rokhlin VI., J. Comput. Phys., 73, 325 (1987).

[44]Schmidt K.E., Lee M.A., J. Stat. Phys., 63, 1223 (1991).

[45]Ding H.Q., Karasawa N., Goddard W.A., J. Chem. Phys., 97, 4309 (1992).

[46]Ewald P.P., Ann. Physik., 64, 253 (1921).

[47]Paddison S. J., Reagor D.W., Zawodzinski T.A. Jr., J. Electroanal. Chem.,459, 91 (1998).

[48]Paddison S. J., Bender G., Kreuer K. D., Nicoloso N., Zawodzinski T.A. Jr., J. New Mat. Electrochem. Syst., 3, 291 (2000).

[49]Paddison S.J., Pratt L.R., Zawodzinski T.A. Jr., J. Phys. Chem. A, 105, 6266 (2001).

[50]Eikerling M., Paddison S. J., Pratt L.R., Zawodzinski T.A. Jr., Chem. Phys. Lett., 368, 108 (2003).